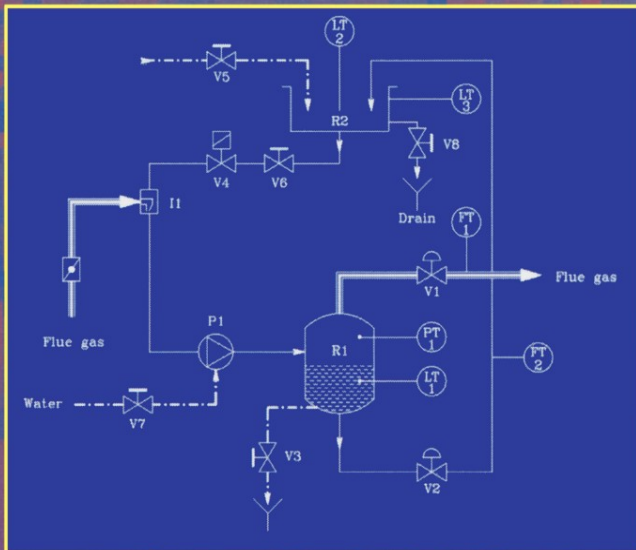Roderick Murray-Smith
Robert Shorten (Eds.)

Switching and Learning in Feedback Systems

European Summer School on Multi-Agent Control
Maynooth, Ireland, September 2003
Revised Lectures and Selected Papers

Springer

Control of Yaw Rate and Sideslip in 4-Wheel Steering Cars with Actuator Constraints[⋆]

Miguel A. Vilaplana, Oliver Mason, Douglas J. Leith, and William E. Leithead

Hamilton Institute
National University of Ireland, Maynooth, Co. Kildare, Ireland

Abstract. In this paper we present a new steering controller for cars equipped with 4-wheel steer-by-wire. The controller commands the front and rear steering angles with the objective of tracking reference yaw rate and sideslip signals corresponding to the desired vehicle handling behaviour. The structure of the controller is based on a simplified model of the lateral dynamics of 4-wheel steering cars. We show that the proposed structure facilitates the design of a robust steering controller valid for varying vehicle speed. The controller, which has been designed using classical techniques according to the Individual Channel Design (ICD) methodology, incorporates an anti-windup scheme to mitigate the effects of the saturation of the rear steering actuators. We analyse the robust stability of the resulting non-linear control system and present simulation results illustrating the performance of the controller on a detailed non-linear vehicle model.

1 Introduction

The concept of generic prototype vehicles has emerged as a promising solution to an outstanding challenge in the development of ride and handling characteristics for advanced passenger cars: the bridging of the gap between numerical simulations based on a vehicle model –a virtual prototype– and experiments on a proof-of-concept prototype vehicle. A generic prototype vehicle would be equipped with advanced computer-controlled actuators enabling it to modify its ride and handling characteristics. Examples of such advanced actuators are four and rear steer-by-wire, brake-by-wire and active suspensions. An integrated chassis controller would command those actuators to track a set of reference signals corresponding to a desired ride and handling behaviour. Currently, moving-base driving simulators are used to emulate the ride and handling behaviour of virtual prototypes prior to building real ones. However, the achievable accelerations of such simulators severely constrain their ability to realistically recreate the full range of vehicle motion. Generic prototype vehicles could allow for the realistic recreation of the ride and handling characteristics of virtual prototypes, thereby enabling engineers to experience and evaluate their behaviour prior to making the decision of building expensive proof-of-concept prototypes.

In this paper, we present a steering controller that enables cars equipped with 4-wheel steer-by-wire to display predefined handling characteristics. This steering controller is intended as a first step towards an integrated chassis controller for a generic prototype vehicle. The proposed steering controller commands front and rear steering angles with the objective of tracking reference yaw rate and sideslip angle signals obtained online from the driver's inputs to steering wheel and pedals. These reference signals describe the lateral dynamic response to those inputs of a virtual prototype with the desired handling characteristics. In addition, the steering controller automatically rejects disturbances in sideslip and yaw rate, such as those caused by μ-split braking manoeuvres or lateral wind gusts. We assume that the controlled output variables, i.e. yaw rate and sideslip angle, are measured (in practice, the latter may typically be estimated using, for example, a Kalman filter).

A substantial body of research on the control of 4-wheel steering cars already exists and a variety of control structures have been proposed in the literature. Most of these structures rely on the use of gain-scheduled feedforward control to command the rear steering angle [1]. In such control structures, some of which have been implemented on production passenger cars, the rear steering angle is computed as a function of the front steering angle that results from the driver's input to the steering wheel. The different control laws depend on the performance objectives, which are usually related to the improvement of the manoeuvrability and cornering stability of the vehicle. The work described in [2] proposes to combine feedforward and feedback control to command the rear steering angle, while the front steering angle remains under direct control of the driver. The control objective is to follow a predefined model of the vehicle dynamics. In order to achieve a satisfactory degree of robustness the feedback controller is designed using μ synthesis. An example of an steering controller specifically designed for cars equipped with 4-wheel steer-by-wire is presented in [3]. The controller structure is based on the cross-feedback of the measured yaw rate to the front steering angle. This structure decouples the control of the lateral acceleration from the control of the yaw rate. Two outer feedback loops are used so that front wheel steering is used to track the desired lateral acceleration and rear wheel steering is used to regulate the damping of the resulting yaw dynamics.

The structure of the steering controller presented in this paper is based on a simplified linear model of the lateral dynamics of 4-wheel steering cars at constant speed. The main elements of the controller structure are a linear input transformation and a speed-dependent inner feedback loop. When applied to the simplified model mentioned above, this structure partially decouples the sideslip and yaw rate responses to the new controllable inputs, with the yaw rate response being speed-invariant. Thus, the proposed structure acts as an implicit gain scheduling on the vehicle speed. The control design is based on a more accurate model of the vehicle lateral dynamics. This model includes the steering actuator dynamics as well as the communication time delay between controller and actuators. When applied to this model, the proposed controller structure results in approximate partial decoupling of the sideslip and yaw rate responses,

with a nearly speed-invariant yaw rate response. The resulting 2-by-2 multivariable control design problem is restated as two single-input, single-output (SISO) control design problems according to the ICD paradigm. Assuming certain bandwidth restrictions, individual linear controllers for the resulting sideslip and yaw rate channels are designed using classical techniques. The resulting steering controller satisfies robustness and disturbance rejection requirements. The controller is augmented with a feedforward element to improve the response to reference inputs and with an anti-windup scheme to mitigate the effects of the saturation of the rear steering actuators. The resulting non-linear steering controller is valid for varying vehicle speed and shows excellent performance robustness to model uncertainty.

Since the proposed steering controller is intended as the foundation for an integrated chassis controller, the main design criteria are transparency, simplicity and modularity. We have adopted the ICD methodology in an attempt to satisfy these criteria. ICD exploits the full potential of diagonal control within a classical Nyquist-Bode framework, opening the way for modular and transparent design based on individual SISO channels that arise naturally from the control specifications. In addition, we deal with the issue, often overlooked in the literature, of ensuring that the steering controller remains robustly stable and performs satisfactorily in the event of rear steering actuator saturation.

In this paper, we focus on describing the controller structure and analysing its robust stability considering the possible saturation of the rear steering actuators. A detailed description of the control design process can be found in [4].

The remainder of this paper is structured as follows. First, we describe the simplified model of the lateral dynamics of 4-wheel steering cars used to define the structure of the proposed steering controller. Based on this model, we derive the controller structure and state the resulting multivariable control design problem. Subsequently, we introduce the ICD methodology in the context of the problem at hand. Next, we apply the proposed controller structure to a more accurate model of the lateral dynamics of 4-wheel steering cars and restate our multivariable control design problem in terms of individual channels according to ICD. Then, we briefly explain the design process. Subsequently, we analyse the robust stability of the resulting non-linear control system using some new results from the theory of common quadratic Lyapunov functions. Finally, simulation results obtained with a detailed non-linear model of a Mercedes S-Class are given to illustrate the performance and robustness of the steering controller.

2   Simplified Linear Model of the Lateral Dynamics of 4-Wheel Steering Cars

Throughout this paper, it is assumed that the essential features of the lateral dynamics of the car can be described using the single-track model [3]. In the single-track model, the two wheels at each axle are lumped into a single imaginary wheel located at the centre of the respective axle. The resulting front and rear wheels are interconnected by a one-dimensional rigid element with the car's

mass and moment of inertia around the vertical axis. The forces acting on each wheel of the single-track model correspond to the combined forces acting on the left and right wheel at the corresponding axle. Only the lateral motion of the car is considered when using the single-track model. It is assumed that the centre of gravity of the single-track model is at road level so that the roll, pitch and heave dynamics can be neglected. Additionally, it is assumed that the longitudinal speed is constant. Figure 1 depicts the single-track model indicating the main elements necessary for the analysis of its lateral dynamics.
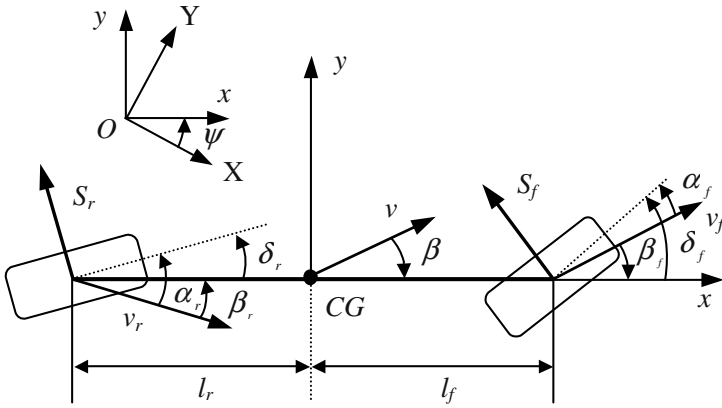

Fig. 1. Single-track model of a 4-wheel steering car

In Fig. 1, the set of reference axes CG-xy, with origin at the centre of gravity CG, is fixed to the vehicle and O-XY is an inertial reference frame; v is the velocity of the vehicle with respect to O-XY; v_f and v_r are the velocities at the front and rear axle, respectively, with respect to O-XY; ψ is the yaw angle and β is the sideslip angle. It is assumed that the front (respectively, rear) steering angle of the single-track model, δ_f (respectively, δ_r) in Fig. 1, corresponds to the steering angle at the two front (respectively, rear) wheels. Since we are not concerned with the longitudinal motion of the single-track model, we only consider tyre-road interaction forces perpendicular to the wheel plane, i.e. cornering forces. The force S_f (respectively, S_r) in Fig. 1 represents the combined cornering forces acting on the front (respectively, rear) axle.

To derive the equations governing the linearised lateral dynamics of the single-track model, we assume that the front and rear steering angles are small, which in turn results in the angles β, β_f, α_f, β_r and α_r in Fig. 1 also being small. Under this assumption, the application of the equations of motion of a rigid body to the single-track model results in

$$\dot{\beta} = \dot{\psi} - \frac{S_f + S_r}{mv_x} \tag{1}$$

$$\ddot{\psi} = \frac{S_f l_f - S_r l_r}{I_{zz}} \tag{2}$$

where m is the mass of the vehicle, I_{zz} is its moment of inertia with respect to the vertical axis, l_f (respectively, l_r) is the distance from the centre of gravity to the front (respectively, rear) axle and v_x is the projection of the velocity vector along the $CG - x$ axis, i.e. the vehicle longitudinal velocity, which we hereafter refer to as the vehicle speed.

For small α_f and α_r, S_f and S_r can be approximated by the following equations [5]:

$$S_f = K_f \alpha_f \tag{3}$$
$$S_r = K_r \alpha_r \tag{4}$$

Considering the kinematics of the single-track model as a rigid body, the angles α_f and α_r are calculated as follows:

$$\alpha_f = \delta_f + \beta - \frac{l_f \dot{\psi}}{v_x} \tag{5}$$

$$\alpha_r = \delta_r + \beta + \frac{l_r \dot{\psi}}{v_x} \tag{6}$$

The constant K_f in (3) is obtained by adequately reducing the combined cornering stiffness of the two front tyres to take into account the caster effect. Conventional steering systems are designed so that the tyre-road contact patch trails behind the steering axis, resulting in a self-aligning torque on the front axle known as the caster effect. We have to consider the caster effect as it is assumed that the front steer-by-wire function is integrated with a conventional steering system. This construction allows for the introduction of a safety management system that reverts to normal steering in case of failure of the steer-by-wire function. The constant K_r in (4) is simply the combined cornering stiffness of the rear tyres. No caster effect is generated at the rear axle since it is assumed that each rear wheel is steered individually by an electro-hydraulic actuator.

Equations (1), (2), (3), (4), (5) and (6) can be rearranged into the state-space representation of a linear time-invariant system with two inputs (δ_f and δ_r) and two outputs (β and $\dot{\psi}$). The resulting state-space representation is given below:

$$\dot{x} = Ax + Bu \tag{7}$$
$$y = Cx + Du \tag{8}$$

where

$$u = \begin{bmatrix} \delta_f \\ \delta_r \end{bmatrix}, \quad y = x = \begin{bmatrix} \beta \\ \dot{\psi} \end{bmatrix}, \tag{9}$$

$$A = \begin{bmatrix} -\dfrac{K_f + K_r}{mv_x} & \dfrac{K_f l_f - K_r l_r}{mv_x^2} + 1 \\[2ex] \dfrac{K_f l_f - K_r l_r}{I_{zz}} & -\dfrac{K_f l_f^2 + K_r l_r^2}{I_{zz} v_x} \end{bmatrix}, \quad B = \begin{bmatrix} -\dfrac{K_f}{mv_x} & -\dfrac{K_r}{mv_x} \\[2ex] \dfrac{K_f l_f}{I_{zz}} & -\dfrac{K_r l_r}{I_{zz}} \end{bmatrix}, \tag{10}$$

$$C = \begin{bmatrix} 1 & 0 \\ 0 & 1 \end{bmatrix} \quad \text{and} \quad D = \begin{bmatrix} 0 & 0 \\ 0 & 0 \end{bmatrix} \tag{11}$$

The matrix transfer function of the system with the state-representation (7)-(8) is given by

$$G(s) = C(sI - A)^{-1}B + D = \begin{bmatrix} g_{11}(s) & g_{12}(s) \\ g_{21}(s) & g_{22}(s) \end{bmatrix} \tag{12}$$

The linear time-invariant system introduced above describes the lateral dynamics of the single-track model around the trajectory given by zero sideslip, zero yaw rate, zero steering angles and constant vehicle speed.

3   Structure of the Steering Controller

The steering controller is to be designed to track reference signals corresponding to normal driving situations. In such situations, the tyres are far from their adhesion limit and the cornering forces behave approximately in a linear fashion according to 3 and 4. The transfer function $G(s)$ in 12 can then be used to model the car lateral dynamics and the design of a steering controller for constant vehicle speed can be tackled by solving the classical 2-by-2 multivariable control design problem depicted in Fig. 2.
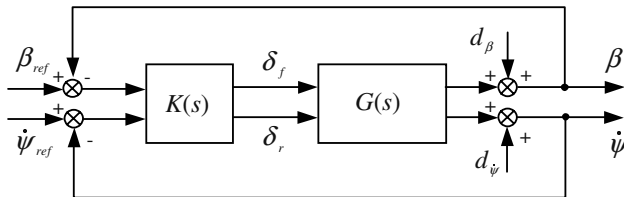

Fig. 2. Design of a linear multivariable steering controller for fixed vehicle speed

A linear controller $K(s)$ designed based on $G(s)$ would only be valid for the corresponding vehicle speed. In principle, a set of local controllers corresponding to different vehicle speeds could be combined using gain-scheduling techniques into a non-linear controller valid for varying vehicle speed. In order to simplify the design process, we take a different approach and state the control design problem in terms of the virtual plant that results from pre-compensating $G(s)$ with a constant matrix gain, i.e. linearly transforming the inputs, and then introducing a speed-dependent matrix gain in a feedback path around the pre-compensated plant. By modifying $G(s)$ in this manner and basing the design on the resulting virtual plant, we impose a structure that facilitates the design of a steering controller valid for varying vehicle speed. This is due to the fact that the virtual plant to be controlled, which we denote as $\tilde{G}(s)$, yields a speed-invariant

yaw rate response. The derivation of the controller structure is explained in detail below.

3.1 Linear Input Transformation

Suppose that the inputs to the plant G(s) are the result of the following linear transformation:

$$\begin{bmatrix} \delta_f \\ \delta_r \end{bmatrix} = E \begin{bmatrix} \Delta_1 \\ \Delta_2 \end{bmatrix} \tag{13}$$

where $E \in \mathbb{R}^{2\times2}$. Considering 3.1, the resulting dynamical equation for the single-track model with respect to the new inputs is:

$$\dot{x} = Ax + BE\Delta = Ax + B_1\Delta, \quad \text{with} \quad \Delta = \begin{bmatrix} \Delta_1 \\ \Delta_2 \end{bmatrix} \tag{14}$$

If we choose

$$E = -\frac{1}{\frac{K_r}{K_f}\left(1+\frac{l_r}{l_f}\right)} \begin{bmatrix} \dfrac{K_r l_r}{K_f l_f} & -\dfrac{K_r}{K_f} \\ -1 & -1 \end{bmatrix} \tag{15}$$

the resulting matrix B_1 is diagonal:

$$B_1 = \begin{bmatrix} -\dfrac{K_f}{mv_x} & 0 \\ 0 & \dfrac{K_f K_f}{I_{zz}} \end{bmatrix} \tag{16}$$

The chosen matrix E correspond to the inputs:

$$\Delta_1 = \delta_f + \frac{K_r}{K_f}\delta_r \tag{17}$$

$$\Delta_2 = \delta_f - \frac{K_r l_r}{K_f l_f}\delta_r \tag{18}$$

A physical interpretation of these new inputs is in terms of a mode given by Δ_1, which excites the sideslip by steering front and rear wheels in the same direction, and a mode given by Δ_2, which excites the yaw rate by steering front and rear wheels in opposite directions. It can be argued that by using Δ_1 and Δ_2 and as control actions the 4-wheel steering vehicle is controlled in a "natural" way, separating the dynamics into their linear and rotational components. The resulting dynamical equation of the yaw rate with respect to the new inputs is:

$$\frac{I_{zz}}{K_f l_f}\ddot{\psi} + \frac{K_f l_f^2 + K_r l_r^2}{K_f l_f v_x}\dot{\psi} = \Delta_2 + \left(1 - \frac{K_r l_r}{K_f l_f}\right)\beta \tag{19}$$

Taking Laplace transforms of both sides in 3.1 and rearranging results in:

$$\dot{\psi}(s) = \frac{K_1}{s + p(v_x)}\Delta_2(s) + \frac{K_1 K_2}{s + p(v_x)}\beta(s) \tag{20}$$

where

$$K_1 = \frac{K_f l_f}{I_{zz}}, \quad K_2 = 1 - \frac{K_r l_r}{K_f l_f}, \quad \text{and} \quad p(v_x) = \frac{K_f l_f^2 + K_r l_r^2}{I_{zz} v_x} \tag{21}$$

The yaw rate dynamics are characterised by a speed-varying first order pole at frequency $p(v_x)$ and are coupled with the sideslip dynamics.

3.2 Speed-Dependent Feedback Element

We introduce a feedback element of the form:

$$\Delta = \tilde{\Delta} - Fy \tag{22}$$

which results in the new vector of controllable inputs $\tilde{\Delta} = \begin{bmatrix} \tilde{\Delta}_1 \\ \tilde{\Delta}_2 \end{bmatrix}$. The matrix $F \in \mathbb{R}^{2 \times 2}$ is given by

$$F = \begin{bmatrix} 0 & 0 \\ K_2 & K_v(v_x) \end{bmatrix} \tag{23}$$

with K_2 from (21) and $K_v(v_x)$ defined as

$$K_v(v_x) = K_0 - \frac{p(v_x)}{K_1} \tag{24}$$

with K_1 from (21) and K_0 an arbitrary constant. Since $y = x$, the state-space equation can be written as follows:

$$\dot{x} = Ax + B_1(\tilde{\Delta} - Fx) = (A - B_1 F)x + B_1 \tilde{\Delta} \tag{25}$$

where

$$A - B_1 F = \begin{bmatrix} -\dfrac{K_f + K_r}{m v_x} & \dfrac{K_f l_f - K_r l_r}{m v_x^2} + 1 \\ 0 & -\dfrac{K_0 K_f l_f}{I_{zz}} \end{bmatrix} \tag{26}$$

The corresponding matrix transfer function with respect to the new controllable inputs is upper-triangular:

$$\tilde{G}(s) = C(sI - \tilde{A})^{-1} B_1 + D = \begin{bmatrix} \tilde{g}_{11}(s) & \tilde{g}_{12}(s) \\ 0 & \tilde{g}_{22}(s) \end{bmatrix} \tag{27}$$

The resulting dynamical equation of the yaw rate with respect to the new controllable inputs $\tilde{\Delta}_1$ and $\tilde{\Delta}_2$ is speed-invariant, taking the form:

$$\ddot{\psi} = -K_0 K_1 \dot{\psi} + K_1 \tilde{\Delta}_2 \tag{28}$$

We choose K_0 to be:

$$K_0 = \frac{K_f l_f^2 + K_r l_r^2}{K_f l_f v_{x0}} \tag{29}$$

with v_{x0} an arbitrary fixed vehicle speed. Then, taking Laplace transforms of both sides of 3.2 results in:

$$\dot{\psi}(s) = \frac{K_1}{s + p(v_{x0})} \tilde{\Delta}_2 \tag{30}$$

The introduction of the feedback element described above results in the yaw rate dynamics depending only on one of the two inputs to be controlled, $\tilde{\Delta}_2$. Besides, the yaw rate response to it is speed-invariant and characterised by a fixed first order pole at frequency $p(v_{x0})$.

3.3   Control Design Problem with Diagonal Controller

Considering the above, we base the control design on the virtual plant $\tilde{G}(s)$. Since we intend to apply the ICD design methodology , we assume that $\tilde{G}(s)$ is to be controlled by a diagonal controller. Consequently, the multivariable control problem in Fig. 2 can be restated as shown in Fig. 3, which depicts the proposed controller structure.
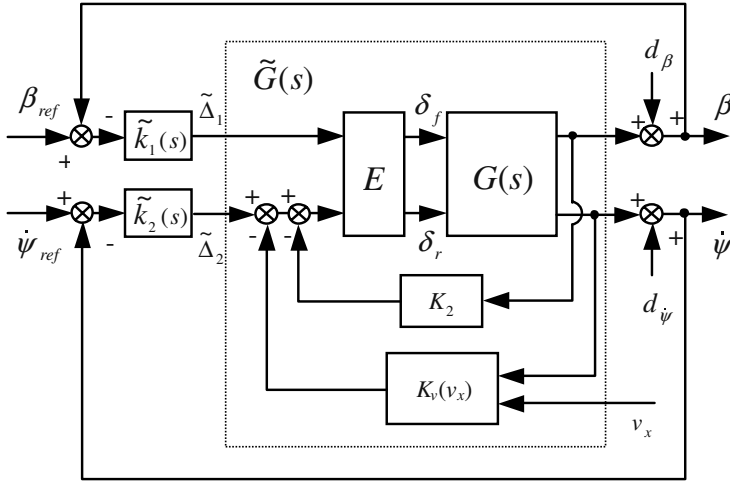

Fig. 3. Multivariable control design problem in terms of $\tilde{G}(s)$

4   Individual Channel Decomposition According to ICD

ICD [6] is a frequency-domain approach to the analysis and design of linear multivariable control systems that provides a solid framework for the application of concepts and techniques from classical linear control, such as Nyquist and

Bode plots and gain and phase margins, to multivariable control design problems. Within the ICD framework, an m-input, m-output feedback system with a diagonal controller is decomposed, without loss of information, into m equivalents SISO feedback control systems called channels. Each individual channel originates from the pairing of a reference input to its corresponding output. Consequently, a channel has its own performance specifications expressed in terms of its response to the corresponding reference input. ICD is very much an application-oriented approach capable of exploring the potential and limitations of diagonal control for a given system. According to the ICD methodology, the multivariable control problem in Fig. 3 can be decomposed into the two channels shown in Fig. 4.
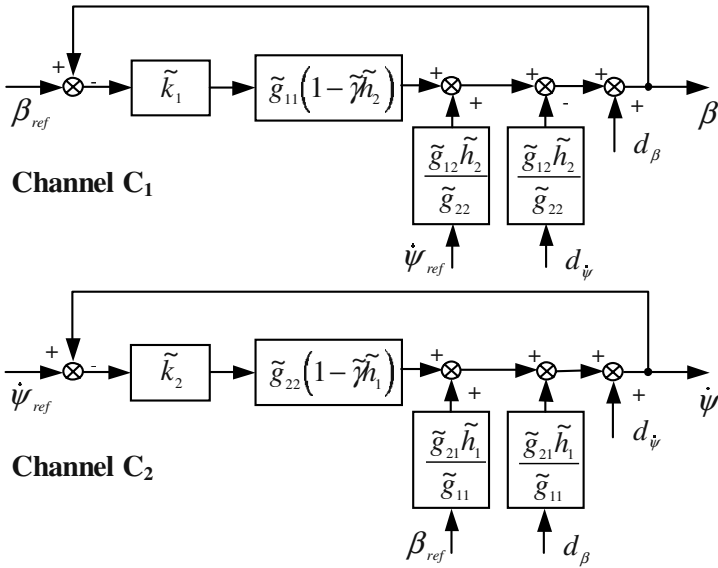

Fig. 4. Multivariable control design problem in terms of $\tilde{G}(s)$

The channel decomposition in Fig. 4 is based on the following functions:

$$\tilde{\gamma}(s) = \frac{\tilde{g}_{12}(s)\tilde{g}_{21}(s)}{\tilde{g}_{11}(s)\tilde{g}_{22}(s)} \tag{31}$$

$$\tilde{h}_1(s) = \frac{\tilde{k}_1(s)\tilde{g}_{11}(s)}{1 + \tilde{k}_1(s)\tilde{g}_{11}(s)}, \quad \tilde{h}_2(s) = \frac{\tilde{k}_2(s)\tilde{g}_{22}(s)}{1 + \tilde{k}_2(s)\tilde{g}_{22}(s)} \tag{32}$$

The closed-loop response of the channels to the reference inputs and $\beta_{ref}(s)$ and $\dot{\psi}_{ref}(s)$ are given by:

$$\beta(s) = \tilde{t}_{11}(s)\beta_{ref}(s) + \tilde{t}_{12}(s)\dot{\psi}_{ref}(s) \tag{33}$$

$$\dot{\psi}(s) = \tilde{t}_{21}(s)\beta_{ref}(s) + \tilde{t}_{22}(s)\dot{\psi}_{ref}(s) \qquad (34)$$

where

$$\tilde{t}_{ii}(s) = \frac{\tilde{c}_i(s)}{1 + \tilde{c}_i(s)}, \quad i = 1, 2 \qquad (35)$$

$$\tilde{t}_{ij}(s) = \frac{\tilde{g}_{ij}(s)\tilde{h}_j(s)}{\tilde{g}_{jj}(s)}(1 + \tilde{c}_i(s))^{-1}, \quad i = 1, 2; \ j = 1, 2; \ i \neq j \qquad (36)$$

The term $\tilde{c}_i(s)$ in 36 and 36 is the open loop transmittance of channel i, which is defined as

$$\tilde{c}_i(s) = \tilde{k}_i(s)\tilde{g}_{ii}(s)(1 - \tilde{\gamma}(s)\tilde{h}_j(s)), \quad i = 1, 2; \ j = 1, 2; \ i \neq j \qquad (37)$$

The closed-loop responses of the channels to the disturbance inputs $d_\beta(s)$ and $d_{\dot{\psi}}(s)$ are as follows:

$$\beta(s) = \tilde{s}_{11}(s)\beta_{ref}(s) + \tilde{s}_{12}(s)\dot{\psi}_{ref}(s) \qquad (38)$$

$$\dot{\psi}(s) = \tilde{s}_{21}(s)\beta_{ref}(s) + \tilde{s}_{22}(s)\dot{\psi}_{ref}(s) \qquad (39)$$

where

$$\tilde{s}_{ii}(s) = \frac{1}{1 + \tilde{c}_i(s)}, \quad i = 1, 2 \qquad (40)$$

$$\tilde{s}_{ij}(s) = -\tilde{t}_{ij}(s) \qquad (41)$$

Robust stability of the multivariable control system is equivalent to the robust stability of the channels providing that the Nyquist plots of the two multivariable structure functions $\tilde{\gamma}(s)\tilde{h}_j(s)$ for $j = 1, 2$ remain far from the (1,0) point.

5 Control Design for a More Accurate Model of the Lateral Dynamics of 4-Wheel Steering Cars

We now consider a more accurate linear model of the car lateral dynamics. We base the design of the linear controllers $\tilde{k}_1$ and $\tilde{k}_2$ on the virtual plant $\tilde{G}(s)$ that results from applying the proposed controller structure (see Fig. 3) to the matrix transfer function of this new model. While still relying on the single-track approximation, we augment the simple model described by (7)-(8) to include the following:

1. The tyre force dynamics and caster effect at the front axle modelled as:

$$\dot{S}_f = a\left(C\left(\delta_f - 2S_f\frac{n_s}{C_L} + \beta - \frac{l_f\dot{\psi}}{v_x}\right) - S_f\right) \qquad (42)$$

where where S_f is the cornering force generated at the front axle, a is a constant that depends on the vehicle speed, C is the nominal tyre cornering stiffness, δ_f is the output of the front steering actuators, n_s is a caster parameter and C_L is an elasticity constant of the steering system.

2. Tyre force dynamics at the rear axle modelled as:

$$\dot{S}_r = a\left(C\alpha_r - S_r\right) \tag{43}$$

where S_r is the cornering force generated at the rear axle.

3. Front and rear steering actuators modelled as second order systems:

$$\begin{bmatrix} \dot{\delta}_f \\ \ddot{\delta}_f \end{bmatrix} = \begin{bmatrix} A_{11}^f & A_{12}^f \\ A_{21}^f & A_{21}^f \end{bmatrix} \begin{bmatrix} \delta_f \\ \dot{\delta}_f \end{bmatrix} + \begin{bmatrix} b_1^f \\ b_2^f \end{bmatrix} \delta_f^i \tag{44}$$

$$\begin{bmatrix} \dot{\delta}_r \\ \ddot{\delta}_r \end{bmatrix} = \begin{bmatrix} A_{11}^r & A_{12}^r \\ A_{21}^r & A_{21}^r \end{bmatrix} \begin{bmatrix} \delta_r \\ \dot{\delta}_r \end{bmatrix} + \begin{bmatrix} b_1^r \\ b_2^r \end{bmatrix} \delta_r^i \tag{45}$$

where δ_f^i and δ_r^i are the input to the front and rear steering actuators, respectively, and δ_f and δ_r are the output of the front and rear steering actuators, respectively.

4. Communication time delay of 20 ms between controller and actuators modelled using Padè approximation.

5.1   Control Specifications

The main requirements for the controlled 4-wheel steering car are:

1. Tracking sideslip and yaw rate reference signals with the highest possible closed-loop bandwidth. These reference signals are obtained in real-time from the driver's inputs to the steering wheel and pedals.
2. Rejecting any disturbances in sideslip and yaw rate with the highest possible bandwidth to avoid interference with the driver's reactions.
3. Maintaining tracking and disturbance rejection performance for vehicle speeds between 10 and 60 m/s and for driving situations involving speed changes, such as acceleration and braking.
4. Robustness with respect to changes in the car parameters, in particular with respect to changes in the tyre stiffness under different road conditions.
5. Satisfactory performance in the event of the saturation of the rear actuators.

5.2   Control Design

We have designed the steering controller considering the more accurate model of the car lateral dynamics introduced above. The model parameters are those corresponding to a Mercedes S Class. Details on the design of the controllers $\tilde{k}_1(s)$ and $\tilde{k}_2(s)$ can be found in [4]. Here we provide a summary of the design process. Before actually designing $\tilde{k}_1$ and $\tilde{k}_2$, two tasks have to be carried out:

1. In order to improve the cross-channel disturbance rejection in the sideslip channel (disturbances from the reference yaw rate to the sideslip response),

a low-pass filter is added to the cross-feedback term. This results in a K_2 in Fig' 3 taking the form:

$$K_2(s) = \left(1 - \frac{K_r l_r}{K_f l_f}\right) \frac{1}{\dfrac{s}{s_0} + 1} \tag{46}$$

where the value of the pole frequency, s_0, is to be selected.
2. The value of v_{x0} in $K_v(v_x)$ has to be chosen. The choice of v_{x0} is related to the robustness of the system.

Once s_0 and v_{x0} have been selected, we can write the transfer function matrix $\tilde{G}(s)$ for any given vehicle speed. With the more accurate model of the car lateral dynamics introduced above, the resulting $\tilde{G}(s)$ is approximately upper-triangular and the yaw rate response can be considered speed-invariant up to a certain frequency. By imposing a bandwidth separation of approximately 7 rad/s between the two channels, the controllers $\tilde{k}_1(s)$ and $\tilde{k}_2(s)$ can be designed based on $\tilde{g}_{11}(s)$ and $\tilde{g}_{22}(s)$, respectively, using classical Bode plot-based SISO techniques. Simple controllers of the form

$$\tilde{k}_1(s) = -\frac{K_{1I}}{s}, \quad \text{Integrator} \tag{47}$$

$$\tilde{k}_2(s) = K_{2p} + \frac{K_{2I}}{s}, \quad \text{PI controller} \tag{48}$$

$$\tag{49}$$

achieve an excellent degree of robustness and satisfactory performance regarding the rejection of cross-channel and external disturbances. These controllers result in a low bandwidth sideslip channel (approx 3 rad/s) and a high bandwidth yaw rate channel (approx 10 rad/s). The speed-dependent feedback term $K_v(v_x)$ acts as an implicit gain scheduling scheme that combines linear controllers parameterised by the vehicle speed into a non-linear controller valid for varying speed.

Having designed $\tilde{k}_1(s)$ and $\tilde{k}_2(s)$ to achieve robustness and disturbance rejection performance, we then add a linear feedforward element to the steering controller to improve its tracking performance. The feedforward element adequately speeds up and shapes the responses to reference signals.

6   Anti-windup Scheme

The steering controller has been designed without considering the possible saturation of the steering actuators. While the maximum allowable front rear steering angle ($\pm 40^0$) is not likely to be reached in the driving situations in which the controller will operate, possible rear actuator saturation has to be considered since the maximum allowable rear steering angle is restricted to only $\pm 5^0$ due to space constraints. When the rear actuators saturate, the feedback loops are broken and the system runs in open-loop because the output of the actuators remain constant independently of the output of the system. Since the steering

controller performs integrating action, the error continues to be integrated and the integral terms may become very large (they "wind up"). This may lead to large transients, excessive overshoots or even instability. An anti-windup scheme has been incorporated into the steering controller to mitigate the effects of the saturation of the rear actuators. The proposed scheme is inspired by conventional anti-windup methods and works as follows. The rear steering angle signal commanded by the controller is subtracted from the average of the measured rear steering angles. The resulting signal is fed back to the input of the controller $\tilde{k}_1(s)$ through a gain K_{AW}. As it will be shown in the simulation results below, this scheme prevents the integrators in both $\tilde{k}_1(s)$ and $\tilde{k}_2(s)$ from winding up and allows the steering controller to retain full control of the yaw rate. Fig. 5 below shows the full steering controller, including feedforward and anti-windup, as it would be implemented in a real car.
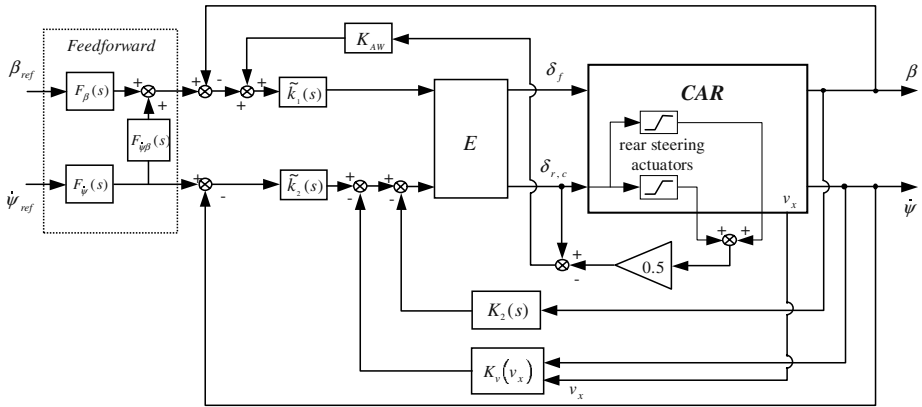

Fig. 5. Full steering controller

7   Robust Stability Analysis

In this section, we analyse the robust stability of the control system considering the possible saturation of the rear steering actuators. In the analysis, we do not consider the feedforward element of the steering controller, as it does not affect the stability of the overall control system, and we use the more accurate model of the car lateral dynamics introduced in Section 5 without the communication time delay. To study the stability of the resulting feedback control system, we transform it into an equivalent one whose forward path contains a SISO linear time-invariant subsystem and whose feedback path contains a saturation nonlinearity. This nonlinearity models the constraints on the rear steering actuators. The equivalent system, which is depicted in Fig. 6, is an example of a Lur'e

system. Thus, asymptotic stability results developed for Lur'e systems, such as the Circle Criterion ([7],[8]), can be used in the analysis.
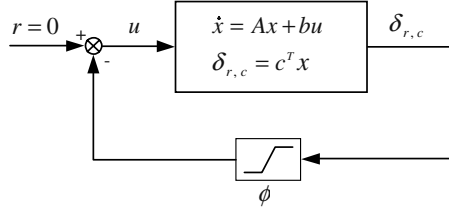

Fig. 6. Equivalent control system for stability analysis: a Lur'e problem

The state space representation of subsystem in the forward path of the feedback system in Fig. 6 is given by:

$$\dot{x} = Ax + bu \tag{50}$$

$$\delta_{r,c} = c^T x \tag{51}$$

where $\delta_{r,c}$ is the rear steering angle demanded by the controller and the matrix $A \in \mathbb{R}^{11 \times 11}$ has the following structure

$$A = \left[\begin{array}{c|c} A_{11} & A_{12} \\ \hline A_{21} & A_{22} \end{array} \right] \tag{52}$$

where the block matrices $A_{11} \in \mathbb{R}^{4 \times 4}$, $A_{12} \in \mathbb{R}^{4 \times 7}$, $A_{21} \in \mathbb{R}^{7 \times 4}$ and $A_{22} \in \mathbb{R}^{7 \times 7}$ are given by

$$A_{11} = \begin{bmatrix} 0 & 1 & -\frac{2}{mv_x} & -\frac{2}{mv_x} \\ 0 & 0 & \frac{2l_f}{I_{zz}} & -\frac{2l_r}{I_{zz}} \\ aC & -\frac{aCl_f}{v_x} & -a(1 + \frac{2Cn_s}{C_L}) & 0 \\ aC & \frac{aCl_r}{v_x} & 0 & -a \end{bmatrix}, \quad A_{12} = \begin{bmatrix} 0 & 0 & 0 & 0 & 0 & 0 & 0 \\ 0 & 0 & 0 & 0 & 0 & 0 & 0 \\ aC & 0 & 0 & 0 & 0 & 0 & 0 \\ 0 & 0 & aC & 0 & 0 & 0 & 0 \end{bmatrix} \tag{53}$$

$$A_{21} = \begin{bmatrix} 0 & -b_1^f E_{12}(K_{2p} + K_v) & 0 & 0 \\ 0 & -b_2^f E_{12}(K_{2p} + K_v) & 0 & 0 \\ 0 & 0 & 0 & 0 \\ 0 & 0 & 0 & 0 \\ Ks_0 & 0 & 0 & 0 \\ -K_{1I} & K_{1I}K_{AW}E_{22}(K_{2p} + K_v) & 0 & 0 \\ 0 & -K_{2I} & 0 & 0 \end{bmatrix} \tag{54}$$

$$A_{22} = \begin{bmatrix} A_{11}^f & A_{12}^f & 0 & 0 & -b_1^f E_{12} & b_1^f E_{11} & b_1^f E_{12} \\ A_{21}^f & A_{22}^f & 0 & 0 & -b_2^f E_{12} & b_2^f E_{11} & b_2^f E_{12} \\ 0 & 0 & A_{11}^r & A_{12}^r & 0 & 0 & 0 \\ 0 & 0 & A_{21}^r & A_{22}^r & 0 & 0 & 0 \\ 0 & 0 & 0 & 0 & -s_0 & 0 & 0 \\ 0 & 0 & 0 & 0 & K_{1I}K_{AW}E_{22} & -K_{1I}K_{AW}E_{21} & -K_{1I}K_{AW}E_{22} \\ 0 & 0 & 0 & 0 & 0 & 0 & 0 \end{bmatrix} \tag{55}$$

The state vector x and the vectors b and c are given by

$$x = \begin{bmatrix} \beta \\ \dot{\psi} \\ S_f \\ S_r \\ \delta_f \\ \dot{\delta}_f \\ \delta_r \\ \dot{\delta}_r \\ K_2 \\ \tilde{u}_1 \\ \tilde{u}_{2I} \end{bmatrix} , \quad b = \begin{bmatrix} 0 \\ 0 \\ 0 \\ 0 \\ 0 \\ 0 \\ -b_1^r \\ -b_2^r \\ 0 \\ -K_{1I}K_{AW} \\ 0 \end{bmatrix} , \quad c = \begin{bmatrix} 0 \\ -E_{22}(K_{2p}+K_v) \\ 0 \\ 0 \\ 0 \\ 0 \\ 0 \\ 0 \\ -E_{22} \\ E_{21} \\ E_{22} \end{bmatrix} \tag{56}$$

The steering angles δ_f and δ_r in the state vector x are the output of the actuators. The state $\tilde{u}_1$ is the output of the controller $\tilde{k}_1$ and the state $\tilde{u}_{2I}$ is the output of the integrator in the controller $\tilde{k}_2$.

The saturation nonlinearity ϕ in the feedback path of the system in Fig. can be modelled as:

$$\phi(\delta_{r,c}) = k_{sat}(\delta_{r,c})\delta_{r,c} \tag{57}$$

with

$$k_{sat}(\delta_{r,c}) = \begin{cases} 1 & \text{if } |\delta_{r,c}| \leq \delta_{sat} \\ \dfrac{\delta_{max}}{|\delta_{r,c}|} & \text{if } |\delta_{r,c}| > \delta_{sat} \end{cases} \tag{58}$$

Here δ_{sat} is the absolute value of the steering angles at which the rear actuators saturate. Note that the function $k_{sat}(\delta_{r,c})$ can be written as a function of the state vector x and $0 \leq k_{sat}(x) \leq 1$ for all x.

The closed-loop state-equation of the system in Fig. 6 can be written as

$$\dot{x} = (A - k_{sat}(x)bc^T)x \tag{59}$$

Now, if there is a positive definite matrix P such that

$$A^T P + PA <, \quad (A - bc^T)^T P + P(A - bc^T) < 0 \tag{60}$$

then $V(x) = x^T Px$ will define a Lyapunov function for the system (59), thus assuring its asymptotic stability. This follows because all of the matrices that

arise in (59) are convex combinations of the two matrices $A, A - bc^T$. Thus if there is a solution P to (60), this guarantees the asymptotic stability of (59).

The Circle Criterion provides a frequency domain condition that can be used to test for the existence of a solution to (60). It has recently been shown that it is also possible to test for the existence of such a solution using a simple time-domain condition ([9],[10]). Specifically, there is a positive definite P satisfying (60) if and only if the matrices A and $(A - bc^T)$ are Hurwitz, i.e. their eigenvalues lie in the open left half of the complex plane, and their product $A(A - bc^T)$ has no negative real eigenvalues. We use this fact to analyse the robust stability of our control system with respect to parametric uncertainty. A major advantage of the time-domain condition is its simplicity, as it only requires the calculation of one set of eigenvalues as opposed to checking a frequency domain condition for infinitely many values of a variable.

Figure 7 summarises the results of the analysis. To generate Fig. 7 we proceeded as follows. First the steering controller was tuned for the nominal values of the car model parameters corresponding to a Mercedes S-Class. The real values of those parameters are uncertain, each of them lying within an interval around its nominal value. For a given fixed vehicle speed, we calculated the entries of A, b and c for a large number of values of the car model parameters randomly chosen from their respective uncertainty intervals. We checked that for all those values of the parameters, the matrices A and $(A - bc^T)$ remained Hurwitz. We then calculated the eigenvalues of $A(A - bc^T)$ for all the values of the parameters considered. We repeated the process outlined above for three different vehicle speeds: 20 m/s, 35 m/s and 50 m/s. In Figure , we plot the two eigenvalues closest to the real negative axis obtained with the different random values of the car model parameters for the three different speeds considered. As it can be seen in the figure, the eigenvalues of the matrix product $A(A - bc^T)$ remain well clear of the real negative axis. In light of the above, we conclude that the control system in Fig. 6 is robustly asymptotically stable for the speeds considered. We can then affirm that our original control system is robustly BIBO stable for those speeds.

8   Simulation Results

The full steering controller has been discretised and implemented on a detailed non-linear simulation model of a Mercedes S-Class equipped with 4-wheel steer-by-wire. The simulation results shown below illustrate the controller's performance and robustness.

8.1   Tracking of Reference Signals at Different Vehicle Speeds

The references to be tracked are as follows:

1. Yaw rate reference: Ramp of slope 0.05 rad/s^2 during 1 s and then maintain constant.
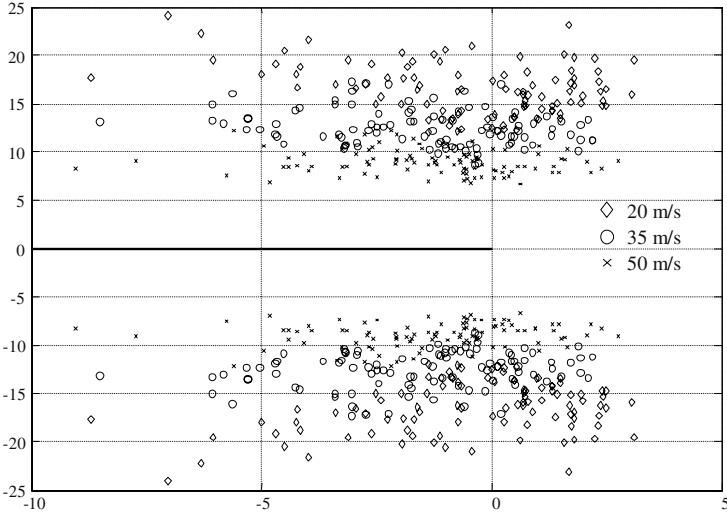
Fig. 7. Illustration of the robust asymptotic stability of the control system

2. Sideslip reference: Ramp of slope -0.005 rad/s during 1 s and then maintain constant.

Figure 8 shows the responses of the control system to these references for different values of the vehicle speed.

8.2   Disturbance Rejection in μ-split Braking

In a μ-split braking situation the car brakes with the tyres at opposite sides of the vehicle on different local road conditions. This results in the tyres at one side of the car see an adhesion coefficient (μ) different from the one seen by the tyres at the other side. An example of μ-split braking is a car braking with the two wheels at one side over a patch of ice and the other two on dry asphalt. In μ-split braking the torque created by the difference between the braking forces at either side of the vehicle introduces disturbances in both yaw rate and sideslip. These disturbances may induce the car to spin and cause the driver to lose control of the vehicle. The proposed steering controller automatically rejects any disturbances in sideslip and yaw rate generated in a μ-split braking situation. To illustrate this capability, consider the following example. A car travels along a straight level road at a speed of 60 m/s. At some point, the driver starts braking without turning the steering wheel. Suppose that the two wheels at the left hand side of the car are on dry asphalt ($\mu \approx 1$) and the two on the right hand side are on ice ($\mu \approx 0.2$). Since the driver keeps the steering wheel straight, the reference signals to be tracked by the steering controller are zero rad/s yaw rate and zero rad sideslip. Figure 9 illustrates the result of
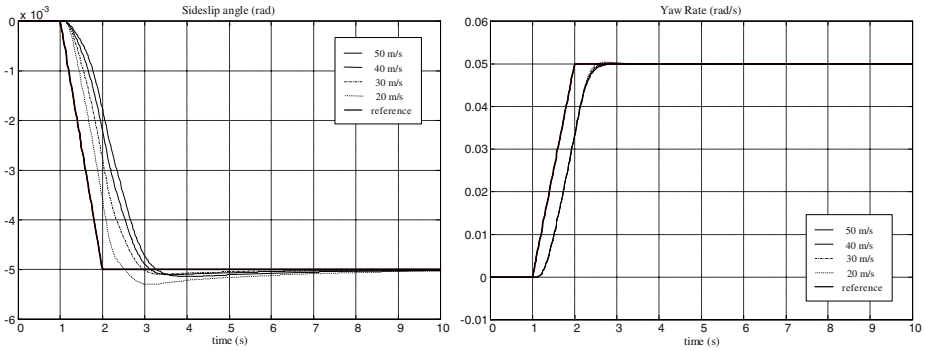
Fig. 8. Tracking performance of the steering controller

simulating this manoeuvre with and without the steering controller switched on. It can be seen that without the steering controller the car spins. On the other hand, with the controller in place the disturbances are quickly rejected and the car barely deviates from its intended straight path. The performance of the steering controller in this manoeuvre demonstrates the robustness of the control system–the cornering stiffness of a tyre during braking decreases as a result of the longitudinal slip [5]–as well as its ability to operate with varying vehicle speed.

8.3   Rear Actuator Saturation

The following manoeuvre is considered. Suppose again that the car travels on a road with a μ-split surface so that the two wheels at the left hand side of the car are on dry asphalt ($\mu \approx 1$) and the two on the right hand side are on ice ($\mu \approx 0.2$). While turning at 50 m/s, the driver applies the brakes moderately for 1 s without moving the steering wheel. The simulation results shown in Fig. 10 below illustrate the response of the controlled car with and without anti-windup. As it can be seen in the figure, the driver applies the brakes between time = 8 s and time = 9 s. The steering controller attempts to automatically reject the disturbances introduced during braking while tracking the reference sideslip and yaw rate signals. This results in the saturation of the rear actuators. Without anti-windup, the controller is not able to recover from the disturbances and spin out of control. On the other hand, the full steering controller (with anti-windup) is able to retain control of the car.

9   Conclusions

In this paper, we have presented a new steering controller for cars equipped with 4-wheel steer-by-wire. The controller allows the car to track given reference
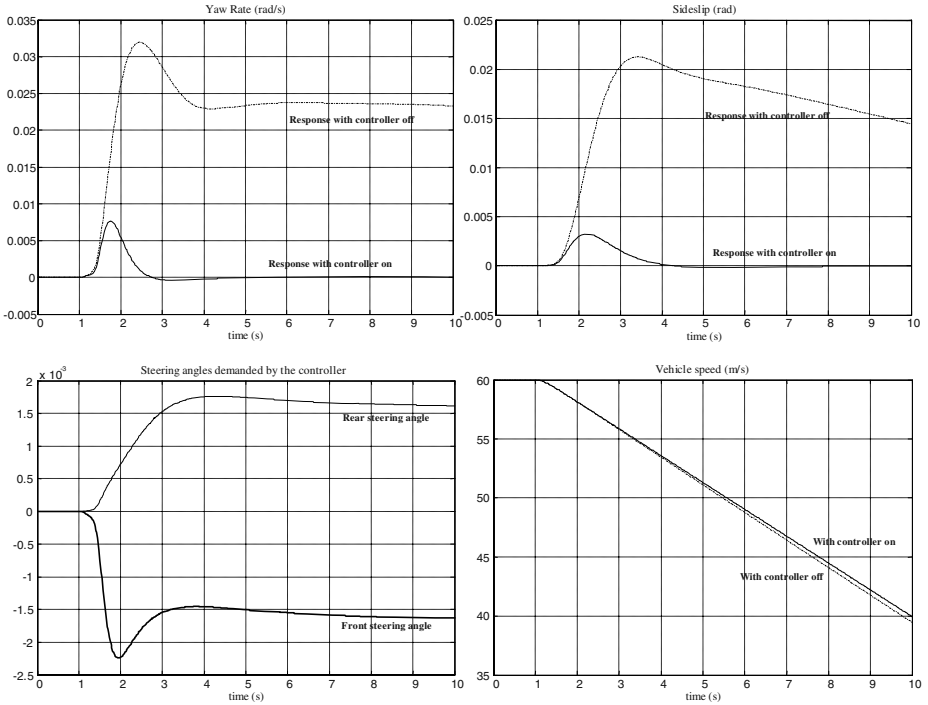
Fig. 9. Disturbance rejection performance of the steering controller in a μ-split braking manoeuvre

sideslip and yaw rate signals while rejecting external disturbances. Schematically, the controller comprises five distinct functional elements: a linear input transformation and a feedback element scheduled with the vehicle speed, which together render the yaw rate dynamics nearly speed-invariant with respect to the new controllable inputs; a linear diagonal controller valid for all operating vehicle speeds, which provides robustness and disturbance rejection performance; a feedforward element, which improves tracking performance; an anti-windup scheme, which allows the controller to perform satisfactorily when the rear actuators saturate. We have analysed the robust stability of the control system using recent results from the theory of common quadratic Lyapunov functions. The performance and robustness of the control system have been demonstrated through simulation. Future work will include a detailed robustness and integrity analysis together with validation experiments with the controller implemented on a real car equipped with 4-wheel steer-by-wire.
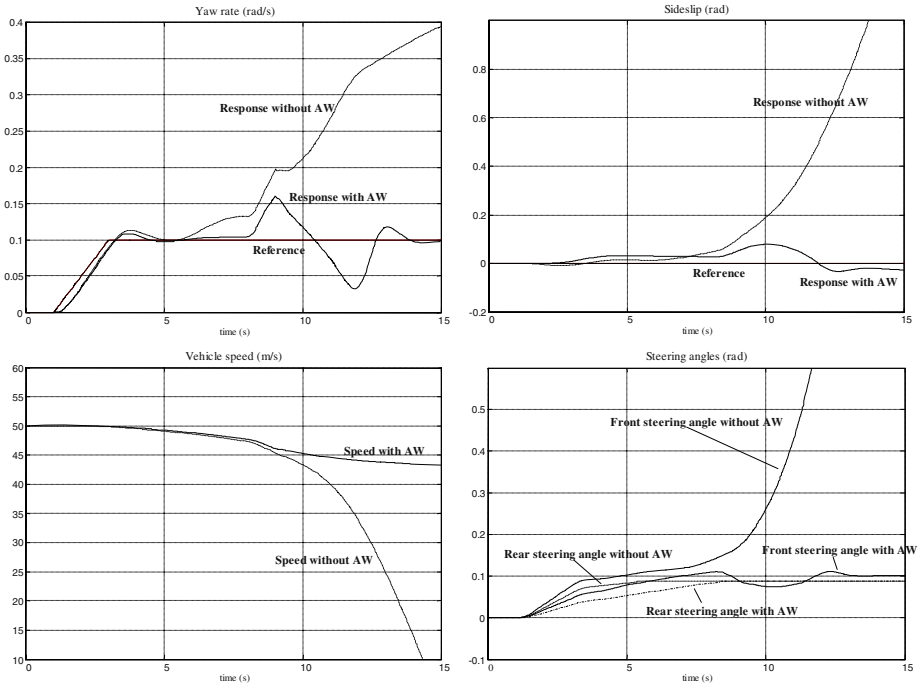
Fig. 10. Performance of the controller when the rear actuators saturate

References

[1] Furukawa, Y., Yuhara, N., Sano, S., Takeda, H., Matsushita, Y.: A review of four-wheel steering studies from the viewpoint of vehicle dynamics and control. Vehicle System Dynamics **18** (1989) 151–186

[2] Hirano, Y., Fukatani, K.: Development of robust active rear steering control. Proceedings of the International Symposium on Advanced Vehicle Control AVEC'96 (1996) 359–376

[3] Ackermann, J.: Robust decoupling, ideal steering dynamics and yaw stabilization of 4WS cars. Automatica **30** (1994) 1761–1768

[4] Vilaplana, M. A., Leith, D. J., Leithead, W. E., Kalkkuhl, J.: Control of sideslip and yaw rate in cars equipped with 4-wheel steer-by-wire. SAE Technical paper 2004-01-2076. Proceeding of the SAE 2004 Automotive Dynamics, Stability and Controls Conference and Exhibition (2004)

[5] Guillespie, T.D.: Fundamentals of vehicle dynamics. Society of Automotive Engineers (1992)

[6] Leithead, W. E., O'Reilly, J.: m-Input m-output feedback control by Individual Channel Design - Part 1: Structural issues. International Journal of Control **56** (1992) 1347-1397

[7] Narendra, K. S., Goldwyn, R. : A geometrical criterion for the stability of certain nin-linear, non-autonomous systems. IEEE Transactions on Circuit Theory **11** (1964) 406–407

[8] Willems, J.: The circle criterion and quadratic Lyapunov functions for stability analysis. IEEE Transactions on Automatic Control **18** (1973) 184

[9] Shorten, R. N., Narendra, K. S.: On common quadratic Lyapunov functions for pairs of stable LTI systems whose system matrices are in companion form. IEEE Transactions on Automatic Control **48** (2003) 618–621

[10] Shorten, R. N., Mason, O., O'Cairbre, F., Curran, P.: A unifying framework for the SISO circle criterion and other quadratic stability criteria. International Journal of Control **77** (2004) 1–8